# Some Current Research in Rotating-Disc Systems

J MICHAEL OWEN AND MICHAEL WILSON

*Department of Mechanical Engineering*
*University of Bath*
*Bath BA2 7AY, UK*

**ABSTRACT: Rotating-disc systems are used to model the flow and heat transfer that occurs inside the cooling-air systems of gas-turbine engines. In this paper, recent computational and experimental research in three systems is discussed: rotor-stator systems, rotating cavities with superposed flow and buoyancy-induced flow in a rotating cavity. Discussion of the first two systems concentrates respectively on pre-swirl systems and rotating cavities with a peripheral inflow and outflow of cooling air. Buoyancy-induced flow in a rotating cavity is one of the most difficult problems facing computationalists and experimentalists, and there are similarities between the circulation in the Earth's atmosphere and the flow inside gas-turbine rotors. For this case, results are presented for heat transfer in sealed annuli and in rotating cavities with an axial throughflow of cooling air.**

## NOMENCLATURE

| | |
|---|---|
| a,b | inner, outer radius of cavity |
| $C_W$ | nondimensional flow rate ($=\dot{m}/\mu b$) |
| $\tilde{g}$ | acceleration |
| G | gap ratio (=s/b) |
| Gr | Grashof number ($=\tilde{g}\, l^3\, \beta\Delta T/\nu^2$) |
| k | thermal conductivity |
| l | characteristic length |
| $\dot{m}$ | mass flow rate |
| Nu | Nusselt number ($=ql/k\Delta T$) |
| Pr | Prandtl number ($=\nu/\alpha$) |
| q | heat flux |
| r, $\phi$, z | radial, tangential and axial coordinates |
| $r_m$ | mean radius of annulus ($=\frac{1}{2}(a+b)$) |

| | |
|---|---|
| Ra | Rayleigh number (=PrGr) |
| $Re_\phi$, $Re_z$ | rotational Reynolds number ($=\Omega b^2/\nu$) , axial Reynolds number ($=Wl/\nu$) |
| Ro | Rossby number ($=W/\Omega a$) |
| s | axial gap between discs |
| T | absolute temperature |
| $V_r, V_\phi, V_z$ | time-averaged radial, circumferential, axial components of velocity |
| W | bulk-average axial velocity |
| $x$ | nondimensional radius (=r/b) |
| $x_a$ | radius ratio of cavity (=a/b) |
| $\alpha$ | thermal diffusivity |
| $\beta$ | $T_{ref}^{-1}$ , volume expansion coefficient |
| $\beta_p$ | pre-swirl ratio ($= V_{\phi,p}/\Omega r_p$) |
| $\Delta T$ | temperature difference |
| $\varepsilon$ | turbulent energy dissipation rate |
| $\Gamma$ | ratio of speed of slower disc to that of faster one |
| $\lambda_T$ | turbulent flow parameter ($= C_w/Re_\phi^{0.8}$) |
| $\rho$ | density |
| $\mu$ , $\nu$ | dynamic viscosity , kinematic viscosity ( $= \mu/\rho$) |
| $\Omega$ | angular speed of cavity |

***Subscripts***

| | |
|---|---|
| b | blade-cooling air |
| d | disc-cooling air |
| I | inlet value |
| o | disc surface |
| p | pre-swirl air |
| ref | reference value |

## 1 INTRODUCTION

Rotating-disc systems are used to represent the flow and heat transfer in the internal cooling-air systems of gas-turbine engines, and Fig. 1 shows a schematic diagram of a typical cooling and sealing system.

The essential features of these complex systems can be modelled using plane rotating and stationary discs, as shown in Fig. 2. It is convenient to classify these systems using the parameter $\Gamma$, which is the ratio of the angular speed of one disc to that of the other: $\Gamma = 0$ is the rotor-stator system; $\Gamma = +1$ is the rotating cavity; $\Gamma = -1$ is the contra-rotating disc system. Contra-rotating discs have been described by Owen[1], and Owen and Rogers[2,3] have described many of the characteristics of rotor-stator systems and rotating cavities. This paper sets out to review recent work on these systems.

In Section 2, the rotor-stator system is discussed. Some areas of current research interest include pre-swirl cooling systems and hot gas ingress from the external mainstream. Section 3 is concerned with the case of a rotating cavity with a peripheral inflow and outflow of cooling air. Buoyancy-induced flow in a rotating cavity, which is discussed in Section 4, has features in common with the flow in the Earth's atmosphere, not least the occurrence of

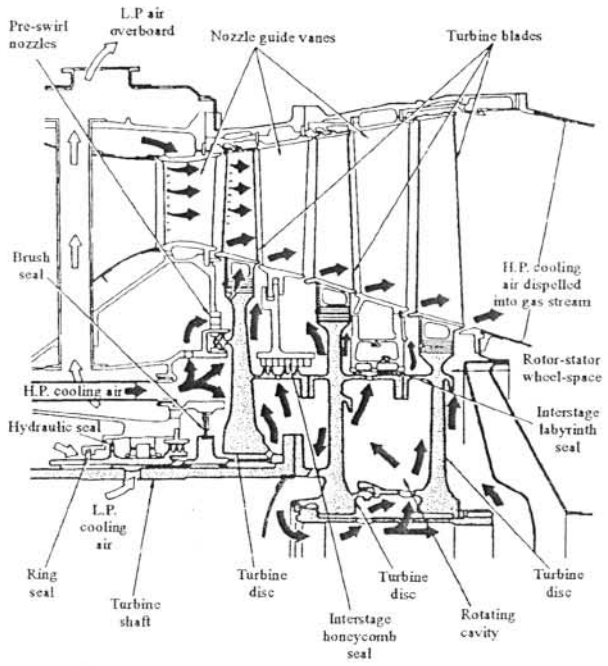


Fig. 1 Schematic diagram of a gas turbine cooling and sealing system (from Rolls-Royce "The Jet Engine")

cyclonic and anti-cyclonic circulations, and it is one of the most difficult problems facing computationalists and experimentalists alike.

## 2 ROTOR-STATOR SYSTEMS

### *2.1 Superposed flows and ingress*

The ingress of hot mainstream gas radially inward into the wheelspace of a gas turbine is a problem of major importance for the turbine designer. In extreme cases, hot-gas ingress can cause overheating, and failure, of the rim of the turbine disc. For the background and a review of ingress, the reader is referred to Owen and Rogers[2] and Johnson *et al.*[4] Recent contributions have been made by Chew *et al.*[5], Reichert and Lieser[6] and Bohn *et al.*[7]

A radial outflow of disc-cooling air can be used to reduce ingress. Wilson *et al.*[8] summarised work which showed that the flow and heat transfer in systems with a superposed radial outflow can be computed with reasonable accuracy using k-ε turbulence models, and some validation of commercial codes has been carried out (Scott *et al.*[9]). In general, heat transfer computations benefit from the use of low-Reynolds-number turbulence models. Iacovides *et al.*[10] tested more sophisticated low-Reynolds-number differential stress models and obtained some improvements to flow-field predictions.

Studies of systems with a superposed radial inflow are also of interest in the ingress context. Iacovides *et al.*[10] tested the Launder-Sharma[11] low Reynolds-number k-ε turbulence model against experimental data for $Re_\phi = 1.47 \times 10^6$ and $C_w = -7389$ (by convention, $C_w < 0$ when the cooling air is directed inward). The empirical Yap correction term for the ε equation, based on near-wall turbulence equilibrium assumptions and which is beneficial for

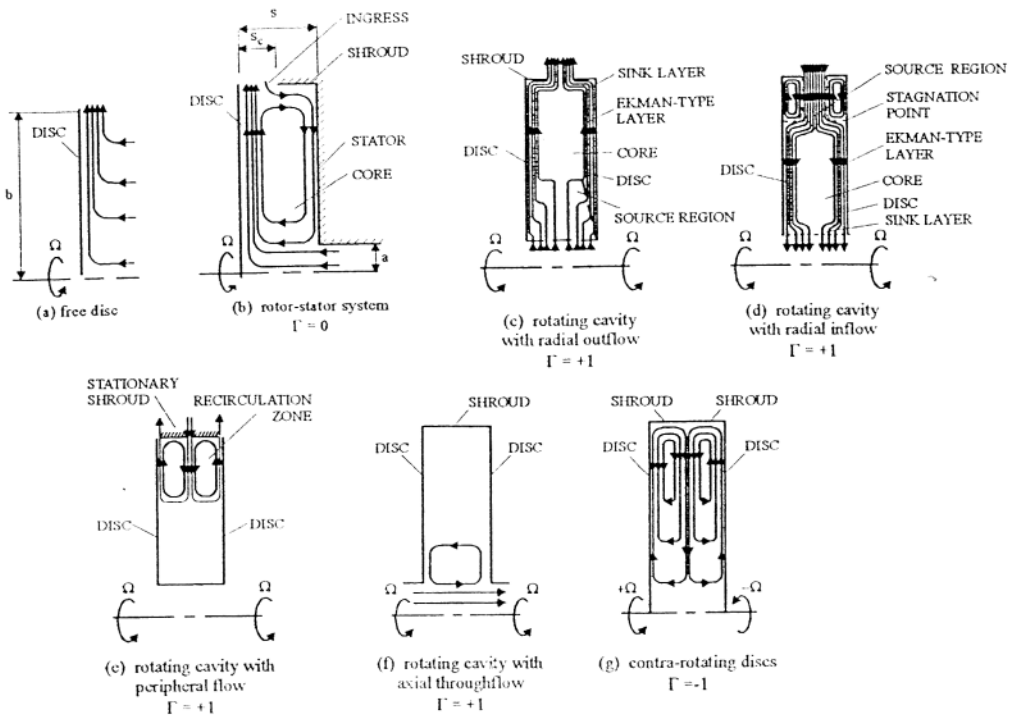


Fig. 2 Schematic diagram of rotating-disc systems

computations without throughflow ($C_w = 0$), behaved badly in the inflow situation, where turbulent flow from the outer part of the system is convected radially inward to less turbulent regions. Further experimental work on radial inflow has recently been completed in Marseille (Gassiat[12]) which may be suitable for the testing of improved computational models.

### *2.2 Pre-Swirl Systems*

Fig. 3a and Fig. 3b illustrate alternative systems used to supply air for the internal cooling of turbine blades through holes near the periphery of the turbine disc. In the "direct transfer" system shown in Fig. 3a, cooling air is delivered, at a high radius, from angled ("pre-swirl") nozzles in a stationary casing. The swirl imparted to the air in the direction of rotation reduces the relative total temperature of the air entering the rotating holes on the disc.

The flow between the discrete stationary pre-swirl nozzles and the blade-cooling holes on the rotating disc is complex, three-dimensional and unsteady. Meierhofer and Franklin[13] measured air temperatures inside rotating blade-cooling holes, and Owen and Rogers[2] reviewed research into direct-transfer systems under adiabatic conditions. Wilson *et al.*[14] summarised some of these findings, and carried out computations and experiments for an idealised direct-transfer rotor-stator system. Axisymmetric steady flow computations (using the Launder-Sharma low-Reynolds-number turbulence model and with annular slots representing the discrete pre-swirl nozzles and blade-cooling holes) consistently under-predicted "blade-cooling air" temperatures measured inside the holes on the experimental rig. The computed mixing (between the pre-swirl cross-flow and a radial outflow of disc-cooling air) is illustrated in Fig. 4, for the pre-swirl chamber formed by inner shrouds and a

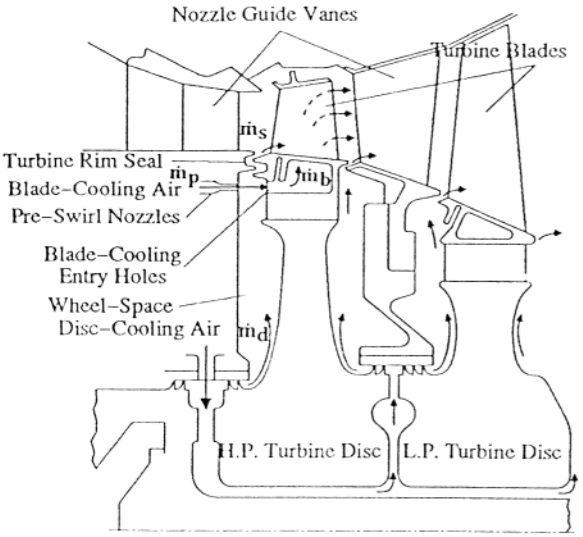


Fig. 3a A direct-transfer pre-swirl system (from Wilson *et al.*[14])

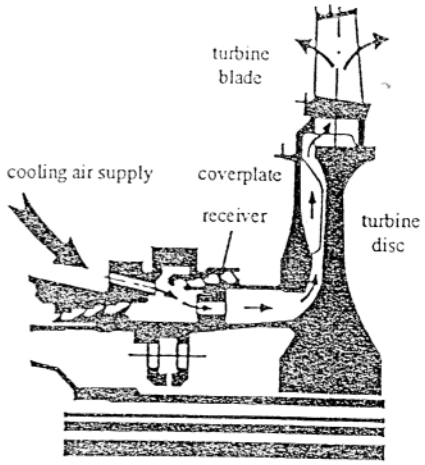


Fig. 3b A cover-plate pre-swirl system (from Popp *et al.*[19])

"rim seal". Table I shows the conditions considered by Wilson et al and comparisons between computed and measured values of $\Delta T$, the change in relative total temperature between the stationary pre-swirl nozzles and the rotating blade-cooling holes. For the direct transfer system, any hot gas ingested via the rim seal can cause serious thermal contamination of the blade-cooling air.

Fig. 3b shows a "cover-plate" system in which air, delivered from pre-swirl nozzles at a low radius, flows radially outward between the turbine disc and a cover-plate attached to it. Ingested mainstream gas is prevented from mixing with the pre-swirl cooling air by a seal at the base of the cover-plate; convective and windage heating of the pre-swirl air will occur as it flows outward over the hot turbine disc.

The flow and heat transfer in cover-plate systems, such as that illustrated in Fig. 3b, has proved tractable to experiment, computation and idealised theoretical analysis. At the high pre-swirl flow-rates expected to occur in engines, Karabay *et al.*[15] found that free-vortex flow occurred in the rotating cavity between the cover-plate and the disc on an experimental rig. Karabay *et al.*[16] used this result to estimate the pressure drop and adiabatic temperature change between the inlet nozzles and the rotating holes. Measured tangential velocities and theoretical pressure distributions were predicted accurately by axisymmetric computations, using similar modelling to that described above for direct-transfer work.

Pilbrow *et al.*[17] described measured and computed heat transfer results for the same cover-plate system. Comparisons between computed and measured Nusselt numbers on the heated disc were reasonably good, however blade-cooling air temperatures were again under-predicted. Fig. 5 shows computed secondary flow streamlines for a typical computation, and Table II gives the results for $\Delta T$ obtained by Pilbrow *et al.* Much of the discrepancy between computations and measurements can be attributed to three-dimensional

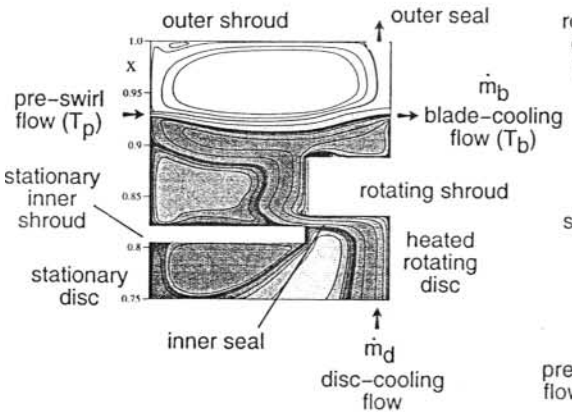


Fig. 4 Computed secondary flows in a direct-transfer system (from Wilson *et al.*[14]) See Table I case 3 for flow conditions

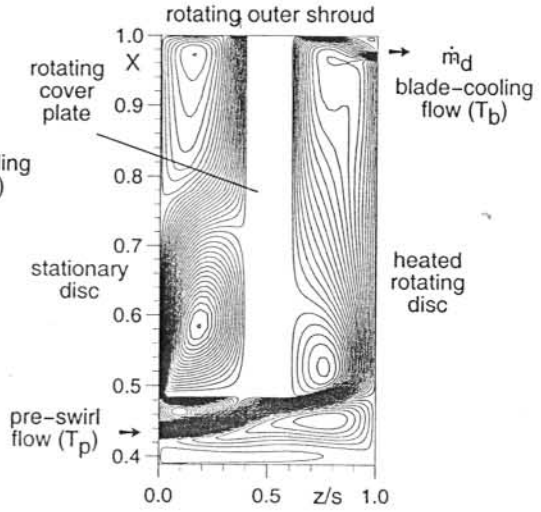


Fig. 5 Computed secondary flows for a cover-plate system (from Pilbrow *et al.*[17]) See Table II case 2 for flow conditions

heat transfer effects close to the discrete holes on the disc, which can be represented by three-dimensional steady models but not by axisymmetric models. The theoretical results for cover-plate systems have been developed further by Karabay *et al.*[18], including an expression for the temperature difference $\Delta T$ in terms of system geometry, the adiabatic work done on the pre-swirl air and the heat transfer from the surface of the disc. The latter term involves the average Nusselt number over the heated disc surface, which is shown to have a minimum value for a particular (optimal) value of inlet pre-swirl for a given system.

Unsteady computational studies of pre-swirl systems (and evaluation of simplified quasi-steady models) are a component of the ICAS-GT integrated research projects now being carried out by European industries and universities, under the Brite-EuRam Framework IV programme (due to be completed in December 2000). The work includes optimisation of pre-swirl nozzle designs, using detailed three-dimensional simulations such as those described by Popp *et al.*[19] for the nozzles in a cover-plate system, and with data provided from complementary experimental research. Cross-validation of commercial CFD codes and standard turbulence models for both flow and heat transfer is an important aspect of this work for the industrial partners.

| $Re_\phi \div 10^6$ | $\beta_p$ | $m_b/m_d$ | $\lambda_T$ | $\Delta T=T_b-T_p$ (comp) | (exp) |
|---|---|---|---|---|---|
| 1.27 | 0.99 | 4.4 | 0.03 | 6.5 | 8.7 |
| 1.27 | 1.98 | 9.0 | 0.03 | -3.4 | -1.7 |
| 1.23 | 0.99 | 2.2 | 0.06 | 2.9 | 6.0 |
| 1.23 | 1.98 | 4.5 | 0.06 | -2.8 | -1.4 |

Table I Blade-cooling air temperature rise in a direct-transfer system (Wilson *et al.*[14])

| $Re_\phi \div 10^6$ | $\beta_p$ | $\lambda_T$ | $\Delta T=T_b-T_p$ (comp) | (exp) |
|---|---|---|---|---|
| 0.535 | 1.110 | 0.173 | 12.2 | 21.9 |
| 1.490 | 1.267 | 0.175 | 11.9 | 16.2 |
| 0.542 | 1.537 | 0.176 | 11.4 | 18.0 |
| 0.898 | 2.049 | 0.351 | 6.6 | 10.6 |
| 0.965 | 2.866 | 0.349 | 6.2 | 6.5 |
| 0.588 | 3.059 | 0.353 | 6.6 | 7.1 |

Table II Blade-cooling air temperature rise in a cover-plate system (Pilbrow *et al.*[17])

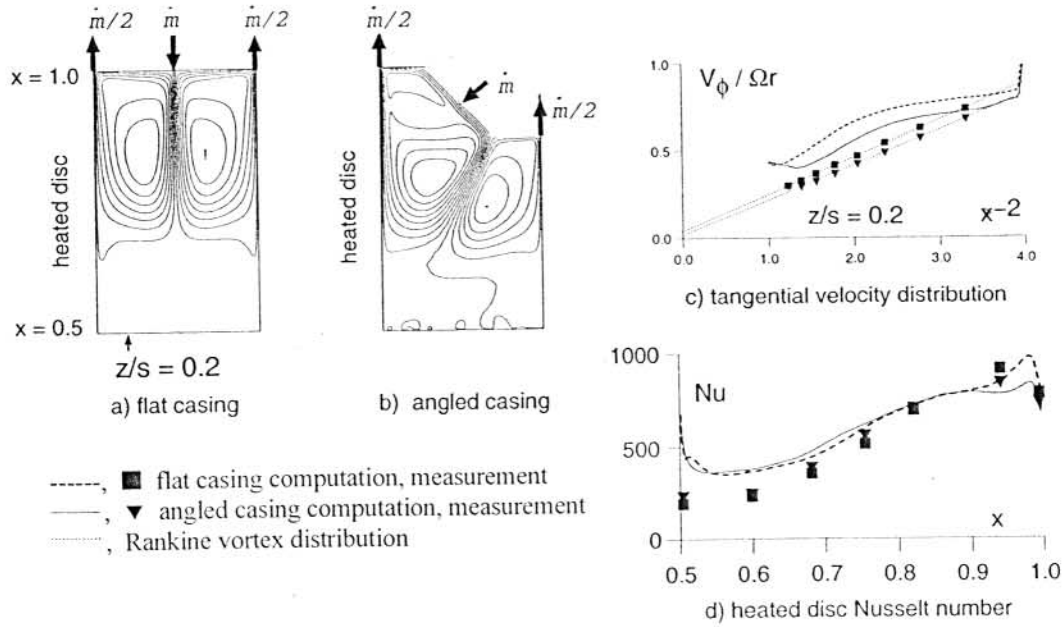


Fig. 6 Flow and heat transfer in a rotating cavity with a stationary outer casing (Jaafar *et al.*[26]) (a/b = 0.5, G = 0.3); $Re_\phi = 1.5 \times 10^6$, $\lambda_T = -0.034$

## 3 ROTATING CAVITY WITH A STATIONARY OUTER CASING

In some gas-turbine cooling systems, a peripheral flow of cooling air is introduced either through nozzles in a stationary casing, as in Fig. 6a,b, or through holes in a rotating disc as in Fig. 7a; the air leaves through clearances in the stationary casing as illustrated. In Fig. 6a, tangential shear at the casing gives rise to flow being pumped radially outward on the discs, resulting in a free shear flow inward between the discs, as shown, and combined free and forced (or Rankine) vortex flow outside the boundary layers (Gan *et al.*[20]). For a closed system (i.e. with no superposed cooling flow) Gan *et al.* found that the inward penetration of the recirculating secondary flows reduced with increasing $Re_\phi$. Increasing the magnitude of the turbulent flow parameter, $\lambda_T$, increased the inward penetration (by convention, $\lambda_T < 0$ when the cooling air is directed inward).

Owen[1] reviewed research into the flow structure in a closed rotating cavity with a stationary flat casing (such as Fig. 6a for $\lambda_T = 0$). The closed system is relevant to the space between rotating components in computer disc drives, and instabilities in the free shear layer can give rise to unsteady three-dimensional flow (see Herrero *et al.*[21]) and Randriamampianina *et al.*[22] as examples of work in the USA and in Europe, respectively). The effect of the superposed peripheral flow on such instabilities has not yet been studied.

Mirzaee *et al.*[23] made heat transfer measurements for the flat casing system with one disc heated (Fig. 6a) and carried out axisymmetric computations, using the Launder-Sharma low-Reynolds-number k-ε turbulence model. Mirzaee *et al.*[24] described a similar study for the stepped-casing configuration (Fig. 7a) and identified different secondary flow recirculations for low or high values of $|\lambda_T|$.

Extensive experimental studies of flow and heat transfer for the angled casing geometry, shown in Fig. 6b and Fig. 7b, have also been carried out at Bath. Axisymmetric

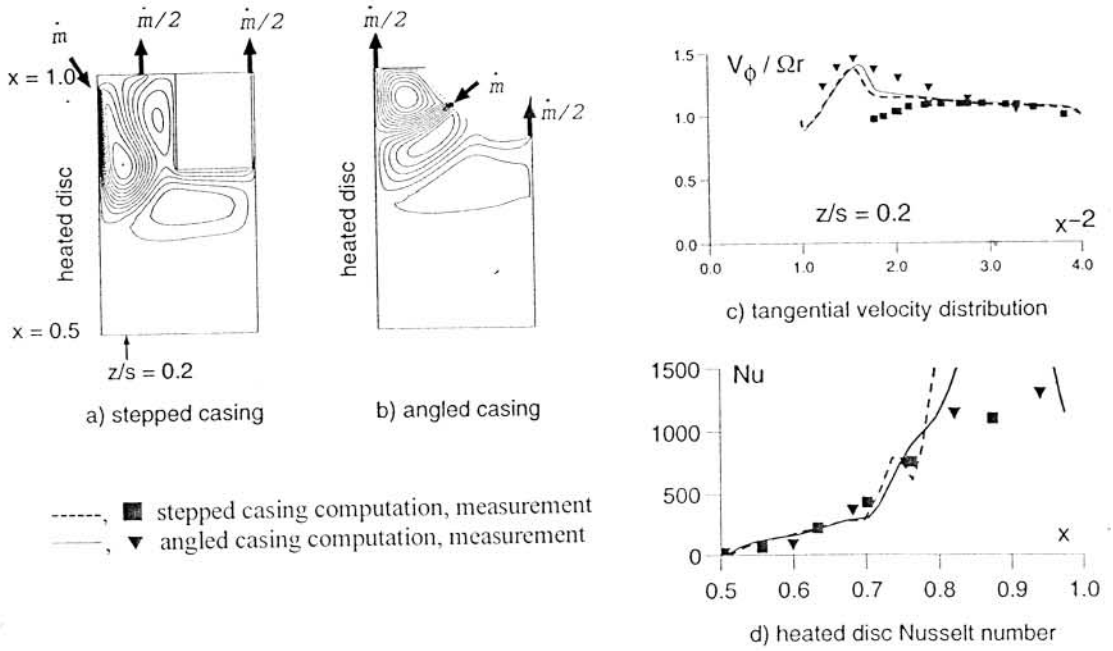


Fig. 7 Flow and heat transfer in a rotating cavity with a stationary outer casing (Jaafar *et al.* [25,26]) (a/b = 0.5, G = 0.3); $Re_\phi = 7.5 \times 10^5$, $\lambda_T = -0.475$

computations for this and the other two systems have been made by Jaafar *et al.* [25,26], using a general-purpose code (PHOENICS) and a high-Reynolds-number k-ε turbulence model with wall-functions. The "flat casing" and "stepped casing" computations confirmed the results of earlier studies. For all of the systems, it was found, both computationally and experimentally, that Nusselt numbers for the heated disc increased with both $Re_\phi$ and $|\lambda_T|$.

Jaafar *et al.*[26] discussed the fluid dynamics for the angled casing configuration, and Fig. 6 shows a comparison of both flow and heat transfer results for the flat and angled casings at one condition, $Re_\phi = 1.5 \times 10^6$ and $|\lambda_T| = 0.034$. For the angled casing, the inlet flow is entrained into the boundary layer on the angled surface (Fig. 6b). The inward shear flow formed where the boundary layers meet at the inner edge of the casing is closely related to that for the "flat casing" in Fig. 6a, as are the secondary flow recirculations. For both configurations, the measured radial distribution of tangential velocity (outside the disc boundary layers) follows a Rankine vortex structure, as described above and shown in Fig. 6c, but this is not reproduced by computations using k-ε turbulence models. This is discussed further by Mirzaee *et al.*[23] Fig. 6d shows that there is little difference between values of Nu for the two systems either for the measurements or the computations.

Fig. 7 shows a comparison of results for the stepped and angled casings at $|\lambda_T| = 0.475$ (and at an inlet swirl ratio close to unity). For "high" values of $|\lambda_T|$ (> 0.1 approx.), Jaafar *et al.*[26] characterised the secondary flows as "inertially-dominated", and in Fig. 7b the powerful inlet flow controls the secondary flow recirculations in the outer part of the cavity. The trend of the measured tangential velocity distribution (at z/s = 0.2), Fig. 7c, is reasonably well predicted for the angled casing configuration. The stepped casing computations, however, show none of the sensitivity to the changes in geometry and inlet location suggested by the measurements.

Heat transfer rates are again very similar for the two configurations, Fig. 7d, and for these cases the computations agree well with the data in the inner part of the system. In the

outer region, the computational results are affected by stagnation of the radial flow on the heated disc surface (separating regions of radially inward and outward flow); the computed location of this region may be inaccurate, due to the deficiencies and simplifications of the axisymmetric model.

The discrepancies between measured and computed velocity distributions illustrated above suggest that the stationary casing problem poses challenges for developers of improved computational and turbulence models for rotating-disc flows. Work is now being carried out in a collaboration between Bath and IRPHE, Marseille, to apply a differential Reynolds-stress turbulence model (Elena and Schiestel[27]) to the closed "flat casing" configuration, for both steady and unsteady flow. The importance of three-dimensional effects, whether caused by instability in the flow or the presence of discrete inlet nozzles for cases involving superposed flow, has not yet been properly addressed.

## 4 BUOYANCY-INDUCED FLOW IN A ROTATING CAVITY

In gas-turbine engines, cooling air often flows through the centre of a stack of rotating compressor discs on its way to the turbine section of the engine. The rotating cavity with an axial throughflow (see Fig. 2f) provides a simple model of the flow between a pair of the corotating compressor discs.

In the absence of a superposed axial throughflow, the temperature differences between the rotating surfaces and the air in the cavity create buoyancy forces, which give rise to free convection. The axial throughflow creates secondary flow, in the form of a toroidal vortex, which interacts with the buoyancy-induced flow. The subsequent flow structure is usually unsteady and three-dimensional, which makes the problem difficult to solve experimentally or computationally. Before studying the axial throughflow case, it is useful to consider the case of a sealed rotating annulus.

### *4.1 Sealed Rotating Annulus*

In a stationary annulus, the gravitational acceleration, g, controls the flow; in a rapidly-rotating annulus (where $\Omega^2 r >> g$), the centripetal acceleration, $\Omega^2 r$ is controlling.

Geophysicists are interested in the case where $\Omega^2 r$ is the same order-of-magnitude as g, which corresponds to the conditions in the Earth's atmosphere. Hide and his co-workers (see, for example, Hide[28,29], Hide and Mason[30], Read[31]) have used the model of an annulus, filled with water and rotating about a vertical axis, to simulate atmospheric flow. When the outer cylindrical surface is hot, the inner surface cold and the two discs adiabatic, then a number of interesting phenomena are observed. For a given value of $\Delta T$ (the temperature difference between the outer and inner cylinders), the structure changes from axisymmetric to "wavy" flow as the rotational speed is increased. When viewed from an axial direction, a sinuous (nonaxisymmetric) stream of fluid meanders circumferentially around the annulus (in a manner similar to that of the jet stream in the atmosphere) transporting heat from the outer to the inner cylinder. Irregular waves, which appear as the speed is increased further, are associated with "geostrophic turbulence" which, unlike turbulence in a stationary frame of reference, tends to be two-dimensional or stratified.

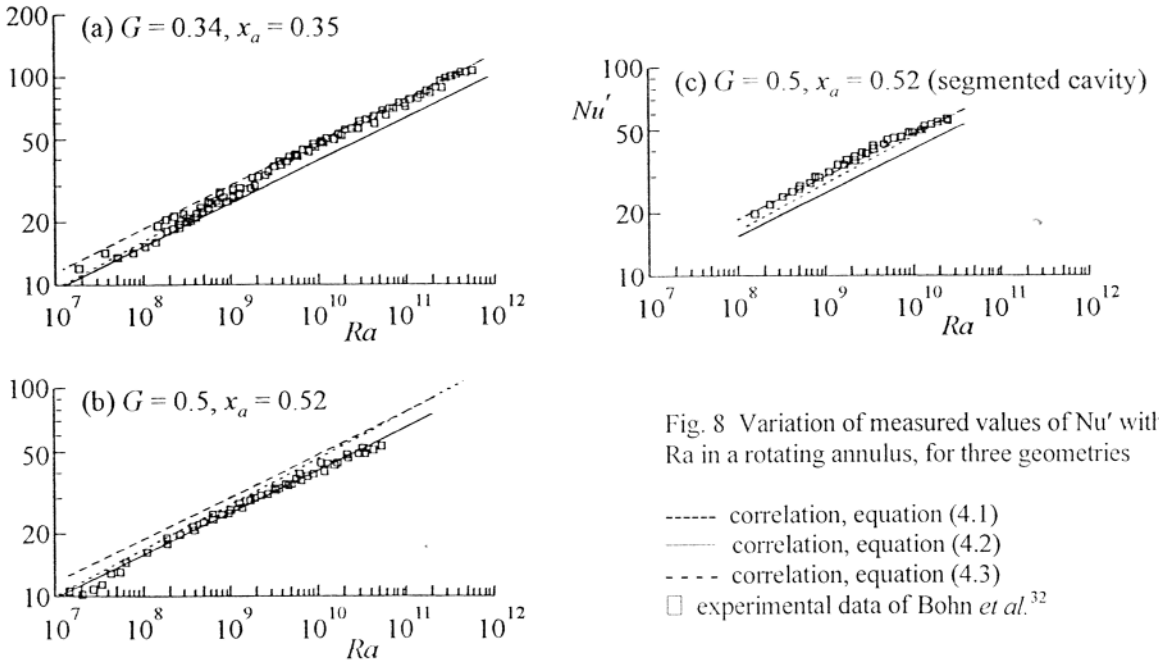


Fig. 8 Variation of measured values of Nu′ with Ra in a rotating annulus, for three geometries

------ correlation, equation (4.1)
——— correlation, equation (4.2)
- - - - correlation, equation (4.3)
□ experimental data of Bohn *et al.*[32]

Although the range of rotational Reynolds numbers and Grashof numbers in geophysical flows are much smaller than those found in gas turbines, some of the flow phenomena are believed to be related.

Bohn *et al.*[32] conducted a combined computational and experimental study for the case of a hot outer cylindrical surface and a colder inner one, and with the two discs insulated. Tests were carried out, for $10^7 < \mathrm{Ra} < 10^{12}$, for three different geometries, and the correlations are given below and shown in Fig. 8.

Geometry A: axisymmetric annulus, $G = 0.34$, $x_a = 0.35$

$$\mathrm{Nu}' = 0.246\ \mathrm{Ra}^{0.228} \tag{4.1}$$

Geometry B: axisymmetric annulus, $G = 0.5$, $x_a = 0.52$

$$\mathrm{Nu}' = 0.317\ \mathrm{Ra}^{0.211} \tag{4.2}$$

Geometry C: annulus with eight 45° segments, $G = 0.5$, $x_a = 0.52$

$$\mathrm{Nu}' = 0.365\ \mathrm{Ra}^{0.213} \tag{4.3}$$

For the above correlations

$$\mathrm{Ra} = 2\,\frac{1-x_a}{1+x_a}\,\mathrm{Pr}\,\beta\Delta T\,\frac{\Omega^2 r_m^2 b^2 (1-x_a)^2}{\nu^2} \tag{4.4}$$

and Nu′ is the ratio of the convective flux to conduction in a stationary fluid. It is interesting to note that for laminar free convection from a stationary surface, $Nu' \propto Ra^{0.25}$, and the above results show no sign of transition to turbulent flow even at values of Ra in excess of $Ra = 10^{11}$. It should also be noted that, for similar conditions in a sealed rotating annulus, the Nusselt numbers for a radial flow of heat are significantly greater than those for an axial flow of heat.

Bohn *et al.*[32] also solved the unsteady, 3D, laminar, elliptic equations for the case of a 45° segment, corresponding to geometry C. The partitions and unheated surfaces were taken to be adiabatic, and two types of heating were used: *axial heat flow* with a hot and a cold disc; *radial heat flow* with a hot outer cylindrical surface and a cold inner one. For the axial heat flow, the computed flow structure reached a steady state in a few seconds of "simulated" time. For the radial heat flow, no steady state was found within the computational time available to the authors. Bohn and Gier[33,34] carried out unsteady 2D and 3D computations, for the 45° segment with a radial heat flow, using the Launder-Sharma low-Reynolds number k-ε turbulence model. They concluded that, compared with the laminar computations, turbulence led to an increase in the average heat transfer and to an increase in the ratio of the local maximum to minimum heat flux on the cylindrical surface.

Bohn *et al.*[35] conducted a combined computational and experimental study for the case of *axial heat flow* in an air-filled rotating annulus. Their measurements were correlated, for $G = 0.5$, $x_a = 0.52$, $2 \times 10^8 < Ra < 5 \times 10^{10}$, by

$$Nu' = 0.346\, Ra^{0.124} \tag{4.5}$$

Their axisymmetric laminar computations were in good agreement with this correlation for $Ra < 2 \times 10^9$. Divergence between computations and measurements at larger values of Ra was attributed to a significant radial flow of heat through the insulated cylindrical surfaces of the experimental rig.

### *4.2 Rotating Cavity with Axial Throughflow*

Vortex breakdown can take place in a swirling, diverging jet of fluid. Under these conditions, which can occur in a rotating cavity with an axial throughflow, the structure of the flow changes dramatically, and formerly steady, axisymmetric flow can become unsteady and three-dimensional. This increases the exchange of fluid between the central jet and the rotating cavity, and it consequently has a strong effect on the heat transfer from the heated surfaces to the cooling air. The radial extent of the recirculation region created by the throughflow tends to decrease as the Rossby number, Ro, and the gap ratio, G, decreases. The reader interested in vortex breakdown is referred to Owen and Pincombe[36] and Farthing *et al.*[37]

Heat transfer tests were conducted for axial throughflow in a number of different rigs (see Farthing *et al.*[37,38]). Flow visualisation revealed that, when the discs were hot and the air cold, the resulting buoyancy-induced flow was nonaxisymmetric. Fig. 9 shows a sequence of photographs taken after (white) smoke had been injected into the air entering the cavity. ("Symmetrical heating" means both discs had the same radial distribution of temperature, and ΔT is the difference between the maximum temperature on the discs and the temperature of the air at inlet to the cavity.) Fig. 9a shows a "radial arm" of smoke; Fig. 9b shows the outline of a cyclonic and anti-cyclonic vortex at the end of the radial arm; Fig. 9c shows the recirculation spreading to most, but not all, of the cavity. The cyclonic (low

(a) $z/s$ = 0.5, $t \simeq$ 2s

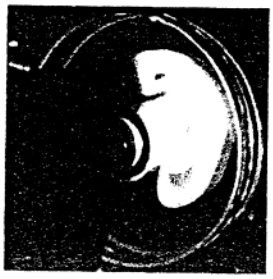

(b) $z/s$ = 0.5, $t \simeq$ 3s

(c) $z/s$ = 0.5, $t \simeq$ 10.5s

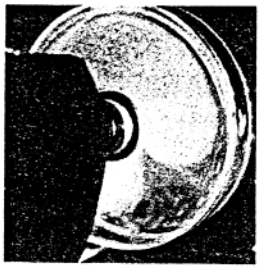

(d) $z/s$ = 0.03

Fig. 9 Photographs of flow structure in a symmetrically heated rotating cavity with axial throughflow: G = 0.267, $Re_z$ = 2180, $Re_\phi$ = 1.3 x $10^4$, $Ro_z$ = 8.4, $\Delta T$ = 55°C, anticlockwise rotation. (Farthing *et al.*[37]) [t is the approximate lapsed time from when the smoke was injected into the air.]

pressure) and anti-cyclonic (high pressure) vortices create the Coriolis forces required for the flow to move radially outward in the radial arm. Velocity measurements showed that the core of fluid between the two discs rotated at a slower speed than the discs themselves, and the difference between the angular speeds of the core and disc, which could be up to 10%, increased as $\Delta T$ and G increased.

For the symmetrically-heated case, Farthing *et al.*[38] correlated their measured local Nusselt numbers on the rotating discs by

$$Nu = 0.0054\, Re_z^{0.30}\, Gr^{0.25} \tag{4.6}$$

where

$$Nu = \frac{q(b-r)}{k(T_0 - T_I)} \tag{4.7}$$

and

$$Gr = \frac{\rho^2 \beta (T_0 - T_I)\Omega^2 r (b-r)^3}{\mu^2} \tag{4.8}$$

Fig. 10 shows the results for G = 0.138, $Re_z = 2 \times 10^4$ and $4 \times 10^5 < Re_\phi < 1.6 \times 10^6$. Also shown are the correlations for free convection for a stationary vertical plate, where for laminar flow

$$Nu = 0.36\, Gr^{0.25} \tag{4.9}$$

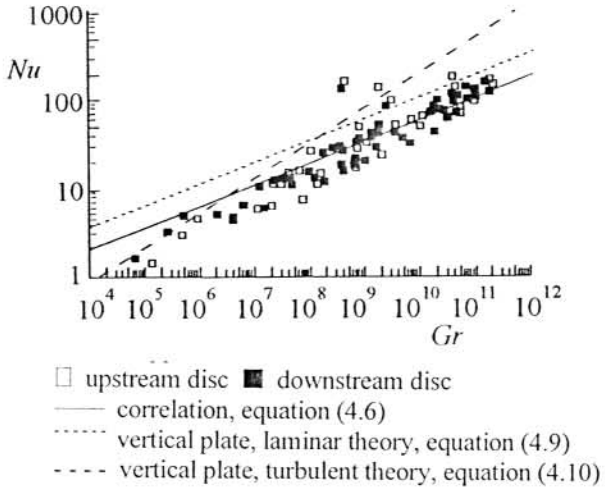


Fig. 10 Variation of Nu with Gr for a symmetrically heated rotating cavity with axial throughflow distribution: G = 0.138, $Re_z = 2 \times 10^4$ experimental data of Farthing *et al*[38].

and for turbulent flow

$$Nu = 0.022\ Gr^{0.4} \tag{4.10}$$

Not surprisingly, the local Nusselt numbers, which were obtained from fluxmeters located at eight radial locations on each disc, show considerable scatter. However, even at Grashof numbers in excess of $10^{11}$, there is no obvious sign of transition from laminar to turbulent flow.

Long[39] and Long and Tucker[40] presented heat transfer measurements for the rotating cavity with a circular inlet for the case where the discs and the peripheral shroud could be heated. They also made measurements of the air temperature inside the rotating cavity, from which they deduced the percentage of axial throughflow that was ingested into the cavity. The percentage depended on the Rossby number: for Ro < 1, around 50% of the throughflow entered the cavity; for Ro > 10, it was around 10%.

Long and Tucker[41] solved the unsteady, 3D, laminar, elliptic equations for one of the geometries studied by Farthing *et al.*, with $Re_\phi = 1.3 \times 10^4$ and $Re_z = 2180$. The computed flow structure, which was three-dimensional and periodic, depended strongly on the radial distribution of the surface temperature of the discs. The computed flow structures were also similar to those observed experimentally by Farthing *et al.*, with radial arms and cyclonic and anti-cyclonic vortices. When the shroud was unheated, the number of radial arms increased from one to two to three as the maximum temperature on the disc was moved radially outward. When the shroud was heated, even more radial arms appeared. The computed flow structure could also change with time: for example, a "one-arm structure" could change to or from a "two-arm structure".

Bohn *et al.*[42] carried out flow visualisation and heat transfer measurements in a rotating cavity with G = 0.2 and a/b = 0.3 for $2 \times 10^5 < Re_\phi < 8 \times 10^5$ and $2 \times 10^4 < Re_z < 7 \times 10^4$. The two discs were heated to produce a radially-increasing temperature distribution with a maximum temperature of 105° C for an air-inlet temperature of 25° C. Their flow visualisation revealed a structure similar to that observed by Farthing *et al.*[37], in which a pair of cyclonic and anti-cyclonic vortices was observed, and the core of fluid rotated at an angular speed around 88% to 90% of that of the discs.

In summary, buoyancy-induced flow tends to be unsteady and three-dimensional. The flow structure comprises a number of cyclonic and anti-cyclonic vortices, and the core of the fluid rotates at a speed slower than that of the discs. Even for values of Gr up to $10^{11}$ (a value associated with turbulent flow in a stationary system), $Nu \sim Gr^{1/4}$ (a correlation usually associated with laminar flow). It is probable that the large Coriolis accelerations suppress or modify the turbulence inside the rotating cavity, and it is unclear that "conventional" turbulent flow occurs at even at the very large Grashof numbers found inside gas-turbine engines. To complicate the above problem even further, an axial throughflow of cooling air can create vortex breakdown which interacts with the buoyancy-induced flow in the cavity.

## 5 CONCLUDING COMMENTS

This paper summarises some recent rotating-disc research having applications to the flow and heat transfer in gas-turbine engines: ingress of hot mainstream gases, pre-swirl cooling-air supply systems and cooling air flows in rotating cavities. It is hoped that the references cited here will adequately direct the interested reader to more details of existing published work. Much further research is currently being carried out for the above systems which should improve the detailed understanding of these complex three-dimensional phenomena.

## References

1. Owen, J. M. (2000) Flow and heat transfer in rotating-disc systems: some recent developments, Proc. 3rd Int. Symp. on Turbulence, Heat and Mass Transfer, Nagoya, pp 33-58
2. Owen, J.M. and Rogers, R.H. 1989. Flow and heat transfer in rotating-disc systems, Vol.1: Rotor-stator systems. Research Studies Press, Taunton. (John Wiley, New York.)
3. Owen, J.M. and Rogers, R.H. 1995. Flow and heat transfer in rotating disc systems: Vol. 2, Rotating cavities. Research Studies Press, Taunton, UK (John Wiley, New York).
4. Johnson, B.V., Mack, G.J., Paolillo, R.E., and Daniels, W.A. (1994). Turbine rim seal gas path flow ingestion mechanisms. AIAA Paper No. 94-2703.
5. Chew, J.W., Green, T., and Turner, A.B. (1994). Rim sealing of rotor-stator wheelspaces in the presence of external flow. ASME Paper No. 94-GT-126.
6. Reichert, A.W. and Lieser, D. (1999). Efficiency of air-purged rotor-stator seals in combustion turbine engines. ASME Paper No. 99-GT-250.

7. Bohn, D., Rudzinski, B., Surken, N. and Gartner, W. (2000). Experimental and numerical investigation of the influence of rotor blades on hot gas ingestion into the upstream cavity of an axial turbine stage. ASME Paper No. 2000-GT-284.
8. Wilson, M., Chen, J. X. and Owen, J. M. (1996) Computation of flow and heat transfer in rotating-disc systems, Trans IMechE 3rd Int Conf on Computers in Reciprocating Engines and Gas Turbines, pp 41-49
9. Scott, R. M., Childs, P. R. N., Hills, N. J. and Millward, J. A. (2000) radial inflow into the downstream cavity of a compressor stator well, ASME Paper No. 2000-GT-0507
10. Iacovides, H., Nikas, K. S. and TeBraak, M. A. F. (1996) Turbulent flow computations in rotating cavities using low-Reynolds-number models, ASME Paper No. 96-GT-159
11. Launder, B.E. and Sharma, B.I., 1974. Application of the energy dissipation model of turbulence to the calculation of the flow near a spinning disc, Letters in Heat and Mass Transfer, **I**, 131-138.
12. Gassiat, M. R. (2000) Etude experimentale d'ecoulements centripetes avec prerotation d'un fluide confine entre un disque tournant et un carter fixe, PhD thesis, Universite de la Mediterranee Aix-Marseille II, France
13. Meierhofer, B. and Franklin, C. J. (1981) An investigation of a preswirled cooling airflow to a gas turbine disk by measuring the air temperature in the rotating channels, ASME Paper No. 81-GT-132
14. Wilson, M, Pilbrow, R. and Owen, J. M. (1997) Flow and heat transfer in a pre-swirl rotor-stator system, J. Turbomachinery, **119**, pp 364-373
15. Karabay, H., Chen, J. X, Pilbrow, R., Wilson, M. and Owen, J. M. (1999) Flow in a "cover-plate" pre-swirl rotating-disc system, J. Turbomachinery, **121**, pp 160-166
16. Karabay, H., Pilbrow, R., Wilson, M. and Owen, J. M. (1999) Performance of pre-swirl rotating-disc systems, ASME Paper No. 99-GT-197
17. Pilbrow, R., Karabay, H., Wilson, M. and Owen, J. M. (1999) Heat transfer in a "cover-plate" pre-swirl rotating-disc system, J. Turbomachinery, **121**, pp 249-256
18. Karabay, H., Wilson, M. and Owen, J. M. (2000) Predictions of effect of swirl on flow and heat transfer in a rotating cavity, Submitted to Int. J. Heat Fluid Flow
19. Popp, O., Zimmermann, H. and Kutz, J. (1998) CFD analysis of coverplate receiver flow, J. Turbomachinery, **120**, pp 43-49
20. Gan, X., Mirzaee, I., Owen, J. M., Rees, D. A. S. and Wilson, M. (1996) Flow in a rotating cavity with a peripheral inlet and outlet of cooling air, ASME Paper No. 96-GT-309
21. Herrero, J., Giralt, F. and Humphrey, J. A. C. (1999) Influence of the geometry on the structure of the flow between a pair of corotating disks, Phys. Fluids **11**, 86-96.
22. Randriamampianina, A., Schiestel, R. and Wilson, M. (1999) Spatio-temporal behaviour in an enclosed corotating disc pair , submitted to J. Fluid Mech.
23. Mirzaee, I., Gan, X., Wilson, M. and Owen, J. M. (1998) Heat transfer in a rotating cavity with a peripheral inflow and outflow of cooling air , J. Turbomachinery, **120**, pp 818-823
24. Mirzaee, I., Quinn, P., Wilson, M. and Owen, J. M. (1999) Heat transfer in a rotating cavity with a stationary stepped casing, J. Turbomachinery, **121**, pp 281-287
25. Jaafar, A. A., Motallebi, F., Wilson, M. and Owen, J. M. (2000) Flow and heat transfer in a rotating cavity with a stationary stepped casing, ASME Paper No. 2000-GT-281
26. Jaafar, A. A., Gan, X., Wilson, M. and Owen, J. M. (2000) Flow in a rotating cavity with a stationary angled casing, Proc. 3rd Int. Symp. on Turbulence, Heat and Mass Transfer, Nagoya, pp 653-660

27. Elena, L. and Schiestel, R. (1996) Turbulence modeling of rotating confined flows, Int. J. Heat Fluid Flow, **17**, 283-289
28. Hide, R. (1977) Experiments with rotating fluids. Quart. J. R. Met. Soc., **103**, 1-28.
29. Hide, R. (1988) Studies of geostrophic turbulence, chaos and other non-linear phenomena in rotating fluids: the role of combined laboratory and numerical experiments. Met. Mag., **117**, 33-34.
30. Hide, R. and Mason, P.J. (1975) Sloping convection in a rotating fluid. Adv. in Phys., **24**, 1, 47-100.
31. Read, P.L. (1988) The dynamics of fluids: the 'philosophy ' of laboratory experiments and studies of the atmospheric general circulation. Met. Mag., **117**, 35-45.
32. Bohn, D., Deuker, E., Emunds, R. and Gorzelitz, V. (1995) Experimental and theoretical investigations of heat transfer in closed gas filled rotating annuli. J. Turbomachinery, **117**, 175-183.
33. Bohn, D. and Gier, J. (1997) The effect of turbulence on the heat transfer in closed gas-filled rotating annuli. ASME Paper No. 97-GT-242.
34. Bohn, D. and Gier, J. (1998) The effect of turbulence in closed gas-filled rotating annuli for different Rayleigh numbers. ASME Paper No. 98-GT-542. (To be published in TransASME.)
35. Bohn, D., Edmunds, R., Gorzelitz, V. and Kruger, U. (1996) Experimental and theoretical investigations of heat transfer in closed gas-filled rotating annuli II. J. Turbomachinery, **118**, 11-19.
36. Owen, J.M. and Pincombe, J.R. (1979) Vortex breakdown in a rotating cylindrical cavity. J. Fluid Mech., **90**, 109-127.
37. Farthing, P.R., Long, C.A., Owen, J.M. and Pincombe, J.R. (1992) Rotating cavity with axial throughflow of cooling air: flow structure. J. Turbomachinery, **114**, 237-246.
38. Farthing, P.R., Long, C.A., Owen, J.M. and Pincombe, J.R. (1992) Rotating cavity with axial throughflow of cooling air: heat transfer. J. Turbomachinery, **114**, 229-236.
39. Long, C.A. (1994) Disk heat transfer in a rotating cavity with an axial throughflow of cooling air. Int. J. Heat Fluid Flow, **15**, 307-316.
40. Long, C.A. and Tucker, P.G. (1994) Numerical computation of laminar flow in a heated rotating cavity with an axial throughflow of air. Int. J. Num. Meth. Heat Fluid Flow, **4**, 347-365.
41. Long, C.A. and Tucker, P.G. (1994) Shroud heat transfer measurements from a rotating cavity with an axial throughflow of air. J. Turbomachinery, **116**, 525-534.
42. Bohn, D.E., Deutsch, G.N., Simon, B. and Burkhardt, C. (2000) Flow visualisation in a rotating cavity with axial throughflow. ASME Paper No. 2000-GT-280.